Figures and figure supplements

C. elegans GLP-1/Notch activates transcription in a probability gradient across the germline stem cell pool

ChangHwan Lee *et al*

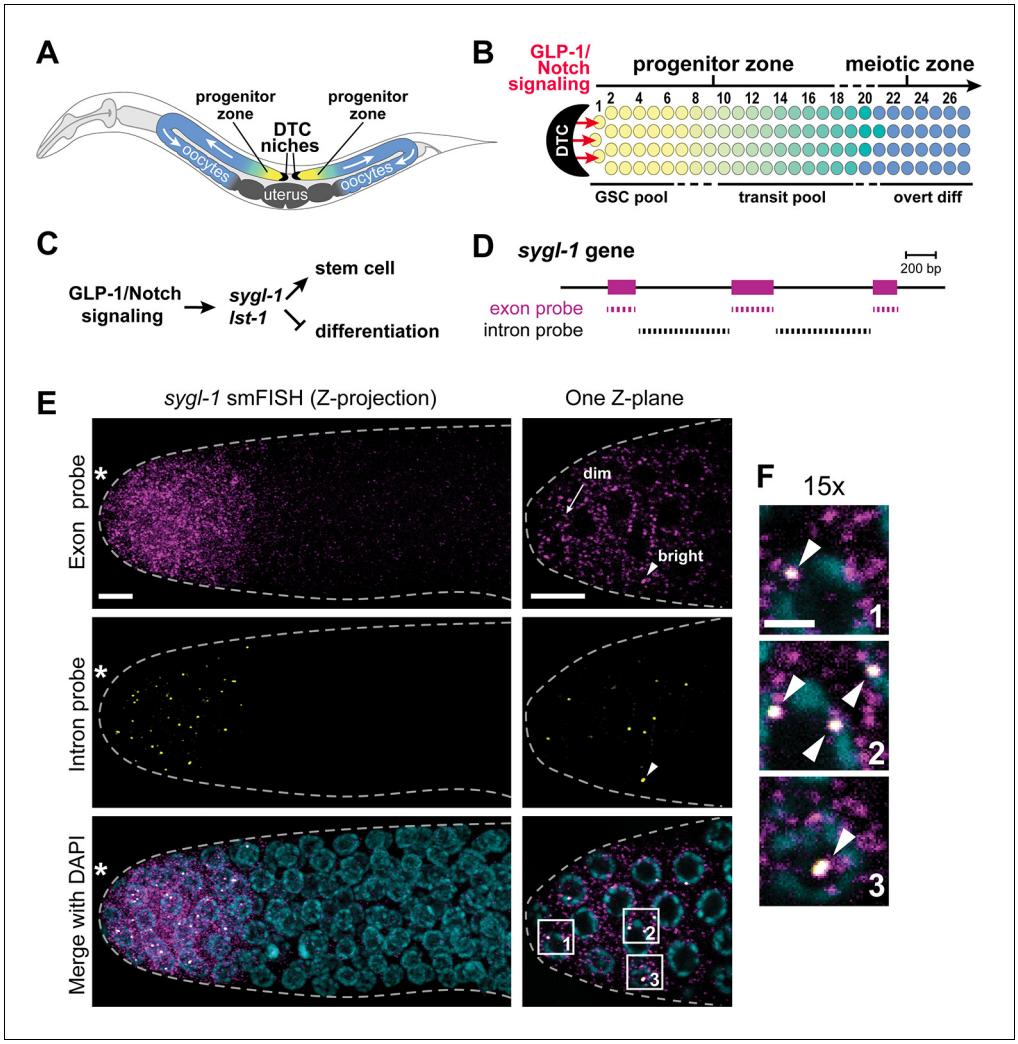

Figure 1. Visualization of *sygl-1* transcripts using smFISH. (**A**) Schematic of adult *C. elegans* hermaphrodite with two U-shaped gonadal arms, each with a single-celled niche (DTC, black crescent) and a progenitor zone of mitotically dividing germ cells at the distal end. Germ cell movement is from distal to proximal (white arrows). Somatic gonadal structures are located centrally (dark grey). (**B**) Organization of germ cells in distal gonad. The only somatic cell in the distal gonad is the DTC; diagrammed here is its cell body (see Introduction for more about DTC architecture). The progenitor zone includes a distal pool of naïve undifferentiated germ cells (yellow), which have been proposed to constitute the GSC pool, and more proximal germ cells (yellow to green transition), which have been triggered to differentiate and are maturing as they transit towards overt differentiation (***Cinquin et al., 2010***). Transit germ cells divide only once or twice before entering the meiotic cell cycle (***Fox and Schedl, 2015***). The boundary between progenitor and meiotic zones is not sharp (dashed line), and similarly, the boundaries of GSC and transit pools are not sharp (dashed lines). Positions of germ cells are conventionally designated as the number of 'germ cell diameters' along the distal-proximal axis from the distal end, with position 1 being immediately adjacent to the DTC cell body; the transition from GSC to transit pools is proposed to occur at position 6–8 (***Cinquin et al., 2010***), and from progenitor to meiotic zone at position 19–22 (***Crittenden et al., 1994***). (**C**) The *sygl-1* and *lst-1* genes are direct targets of GLP-1/Notch signaling and key regulators of germline stem cell maintenance (***Kershner et al., 2014***). (**D**) Schematic of *sygl-1* exon/intron structure. Exon-specific (magenta) and intron-specific (black) probes for single-molecule RNA FISH (smFISH) were labeled with different fluors (see Materials and methods). (**E-F**) *sygl-1* smFISH in distal gonad. Exon probes (magenta); intron probes (yellow). DAPI marks nuclei (blue). Nuclei have DAPI-free centers because of their large nucleoli. Merge (bottom) is an overlay of exon probe, intron probe and DAPI channels. ***Figure 1—figure supplement 1A*** shows *sygl-1* smFISH in a whole gonad. (**E**) Distal gonad dissected from wild-type adult (24 hr post mid-L4 stage), showing dim spots in the cytoplasm (arrow) and bright spots in the nucleus (arrowhead). Grey dashed line marks gonadal outline; asterisk marks distal end of gonad; scale bar is 5 μm. (**F**) 15X magnification of nuclei within boxes in

Figure 1 continued on next page

Figure 1 continued

Figure 1E, bottom panel. The merged images show overlap of exon and intron signals as white spots (arrowheads), which not only overlap with DAPI, as shown here, but are also within nuclei as assayed using a nuclear lamin (***Figure 1—figure supplement 1B***). Scale bar: 2 μm. The specificity of smFISH probes is confirmed in ***Figure 1—figure supplement 1C,D*** and Notch dependence of smFISH signals in ***Figure 1—figure supplement 2***.

DOI: 10.7554/eLife.18370.002

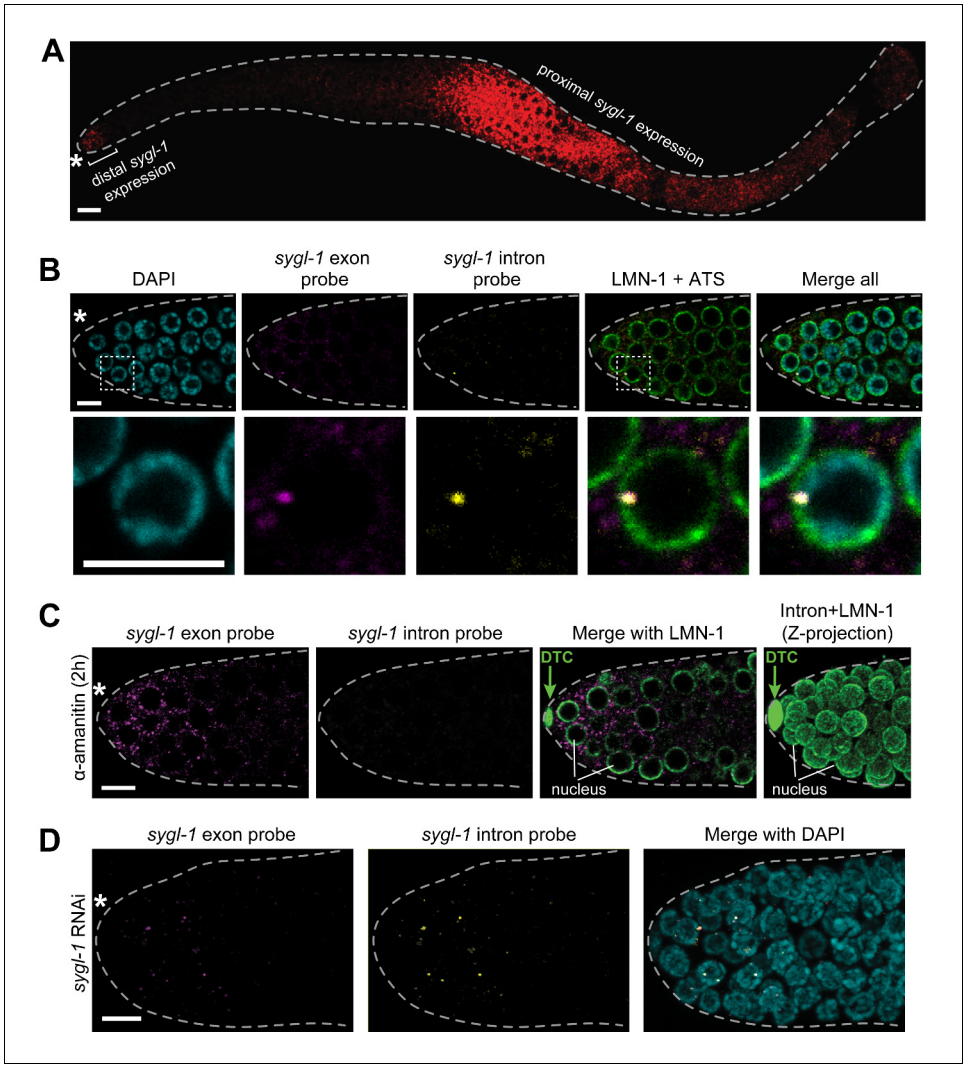

Figure 1—figure supplement 1. *sygl-1* smFISH visualization of nascent nuclear transcripts and mature cytoplasmic transcripts. (**A**) *sygl-1* smFISH using exon probe set shows RNAs (red) in both the distal and proximal regions of a wild-type dissected gonad, as seen previously with conventional *in situ* hybridization (***Kershner et al., 2014***). The proximal *sygl-1* expression is not GLP-1/Notch dependent (***Kershner et al., 2014***) and was not pursued further in this work. Asterisk, distal end; grey dashed line, gonadal outline; scale bar, 20 μm. One Z-plane is shown. (**B-D**) *sygl-1* smFISH in distal gonad dissected from an adult (24 hr post mid-L4 stage), stained as in ***Figure 1E***. Exon probes (magenta); intron probes (yellow); DAPI (blue). Grey dashed line, gonadal outline; asterisk, distal end of gonad; scale bar, 5 μm. (**B**) Gonad stained with *sygl-1* exon and intron probes plus an α-LMN-1 antibody against nuclear lamin to highlight nuclear boundaries (green). Bottom row, 20X magnification of boxed region in top row. One Z-plane is shown. (**C**) Gonad after a 2 hr treatment with 100 μg/ml α-amanitin and stained with *sygl-1* exon and intron probes plus α-LMN-1 antibody staining (green). Left and middle, a single Z-plane. Right, Z-projection of intron probes with LMN-1. DTC, nucleus of DTC. (**D**) Gonad from an animal whose mother was treated with *sygl-1* RNAi at L4 stage. Z-projection is shown.

DOI: 10.7554/eLife.18370.003

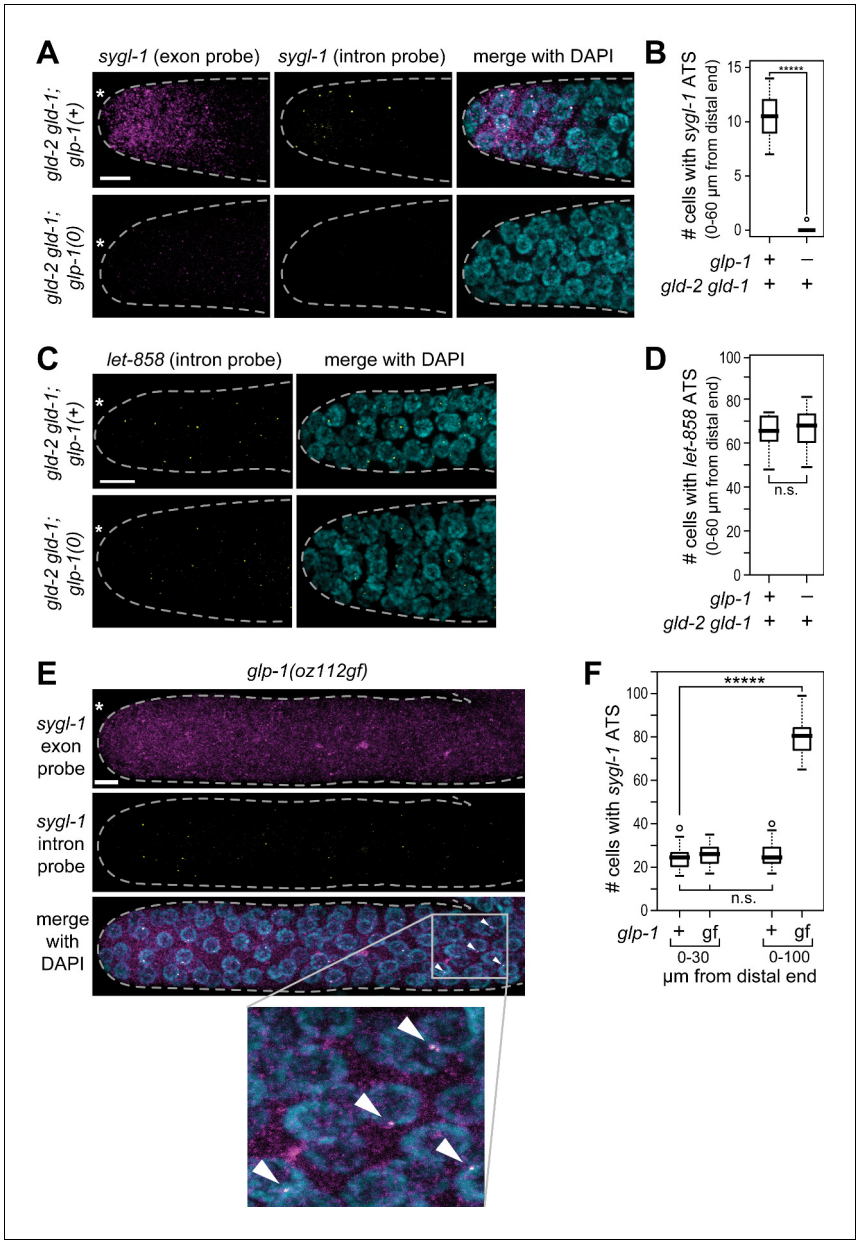

Figure 1—figure supplement 2. GLP-1/Notch-dependence of *sygl-1* ATS. (**A**,**C**,**E**) Z-projections of distal gonads stained using smFISH to *sygl-1* (**A**,**E**) or *let-858* (**C**). Exon probes (magenta); intron probes (ATS; yellow); and DAPI marks nuclei (blue). Conventions and scale as in ***Figure 1E***. (**B**,**D**,**F**) number of germ cells with *sygl-1* ATS (**B**,**F**) or *let-858* ATS (**D**). *****p<0.00001; n.s.: not significant by t-test. For *gld-2 gld-1* and *gld-2 gld-1; glp-1(0)*, n = 16 (**B**, **D**); for *glp-1(oz112gf)*, n = 10 (**F**); for wild-type, n = 21 (**F**). For box-and-whisker plots, the bold line in the box shows the median; top and bottom of box are the third and first quartiles, respectively; whiskers, maximum and minimum of data points; circles, outliers (value greater than 1.5X first or third quartile from the median). (**E**) Arrowheads mark ATS in proximal gonad.

DOI: 10.7554/eLife.18370.004

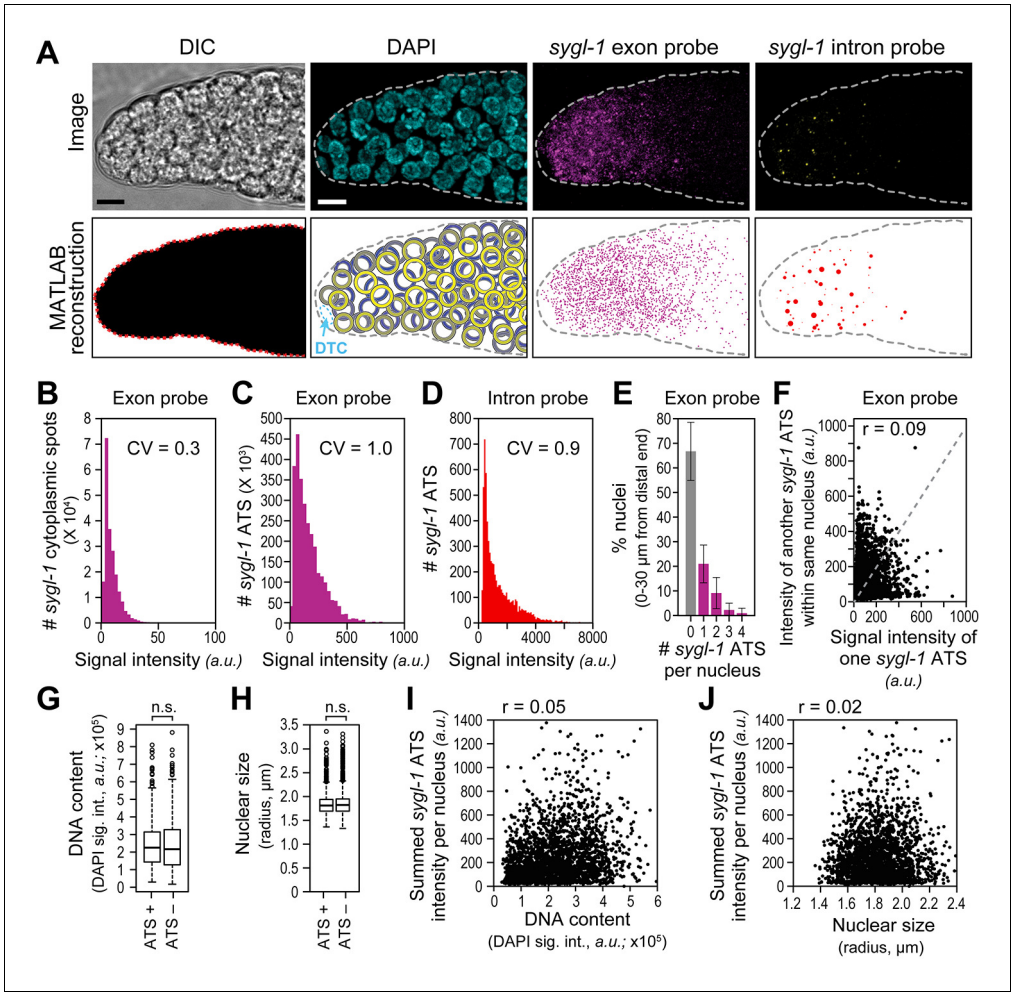

Figure 2. The *sygl-1* transcriptional response to Notch signaling. (**A**) MATLAB reconstruction of distal gonad. Top row, DIC image is one Z-plane; all others are Z-projections. Far left, DIC was used to determine gonadal outline; middle-left, DAPI reveals nuclei (blue); middle-right, signal from *sygl-1* exon probes shows *sygl-1* cytoplasmic mRNAs and nuclear active transcription sites (ATS) (magenta); far right, signal from *sygl-1* intron probes show only ATS (yellow). Bottom row, outputs from custom MATLAB code (***Source code 1***). Far left, gonadal outline (red dashed line), middle-left, germ cell nuclei false-colored in a depth gradient (yellow-blue) according to Z-position and with DTC (cyan) excluded; middle-right, cytoplasmic mRNAs (magenta) with nuclear ATS excluded computationally; far right, ATS (red) with smFISH signals scaled according to intensity. Scale bar: 5 µm. (**B**) Signal intensities of cytoplasmic dots from *sygl-1* exon probes. A total of 222,260 spots were analyzed from 78 gonads. Raw values from Z-planes were normalized to background levels in the same plane and the mean intensity value set to 10 arbitrary units (*a.u.*) for each gonad. CV: coefficient of variation (CV <1, significantly narrow distribution). (**C,D**) Signal intensities of *sygl-1* ATS. A total of 2627 spots were analyzed from 78 gonads. (**C**) Intensities of *sygl-1* ATS using exon probes. We first normalized raw values to background levels in the same Z-plane and then normalized to mean intensity of *sygl-1* cytoplasmic spots seen with the same probe in the same gonad. Mean intensity of *sygl-1* ATS was 172.0 *a.u.*, or roughly 17-fold more than the mean intensity of *sygl-1* individual mRNAs. (**D**) Intensities of *sygl-1* ATS using intron probes. Raw values were normalized to background levels in the same Z-plane. (**E**) Number of *sygl-1* ATS per nucleus in 7018 nuclei (78 gonads). Error bars: standard deviation. (**F**) Pairwise comparisons of *sygl-1* ATS intensities within one nucleus (78 gonads), using normalized values from exon probe. Each black dot represents one pairing. Grey dashed line indicates a perfect correlation (Pearson's correlation coefficient r = 1); r indicates the correlation coefficient from data in the graph. (**G-J**) *sygl-1* transcriptional activity is independent of cell cycle stage. The cell cycle stage was monitored for DNA content (summed DAPI signal) or nuclear size, which are correlated (***Figure 2—figure supplement 1A***), in all nuclei located 0–30 µm (1–7 gcd) from the distal end (n = 6979 nuclei total); n.s.: not significant (p>0.05) by t-test. The cell cycle is also independent from nuclear location in the gonad (***Figure 2—figure supplement 1B,C***). (**G,H**) DNA content (**G**) or nuclear size (**H**) was compared between ATS-positive and ATS-negative cells. For all box-and-

Figure 2 continued on next page

Figure 2 continued

whisker plots in this study, the bold line in the box shows the median; top and bottom of box are the third and first quartiles, respectively; whiskers, maximum and minimum of data points; circles, outliers (value greater than 1.5X first or third quartile from the median). (**I, J**) Summed *sygl-1* ATS intensity was estimated by pooling all ATS signal intensities (*a.u.*) within the same nucleus. Each black dot represents a single nucleus.

DOI: 10.7554/eLife.18370.005

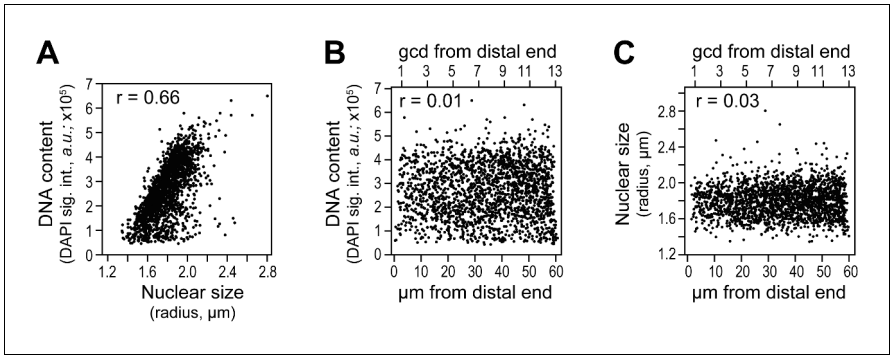

Figure 2—figure supplement 1. Cell cycle analysis in reconstructed gonads. DNA content was estimated as total DAPI signal intensity in a 3-D reconstructed spherical nucleus, and nuclear size as the radius of a 3-D reconstructed spherical nucleus. Each dot in the scatter plots represents a single nucleus. Pearson's correlation coefficient (r) is shown in each plot (r values approaching 0 indicate no correlation while r values approaching 1 indicate a strong correlation). (**A-C**) DNA content and nuclear size were assessed in all germ cell nuclei located 0–60 µm (1–13 gcd) from the distal end in 78 wild-type adult gonads (15,468 nuclei total). (**A**) DNA content is plotted against nuclear size of corresponding nucleus. (**B,C**) DNA content (**B**) or nuclear size (**C**) as a function of position.
DOI: 10.7554/eLife.18370.006

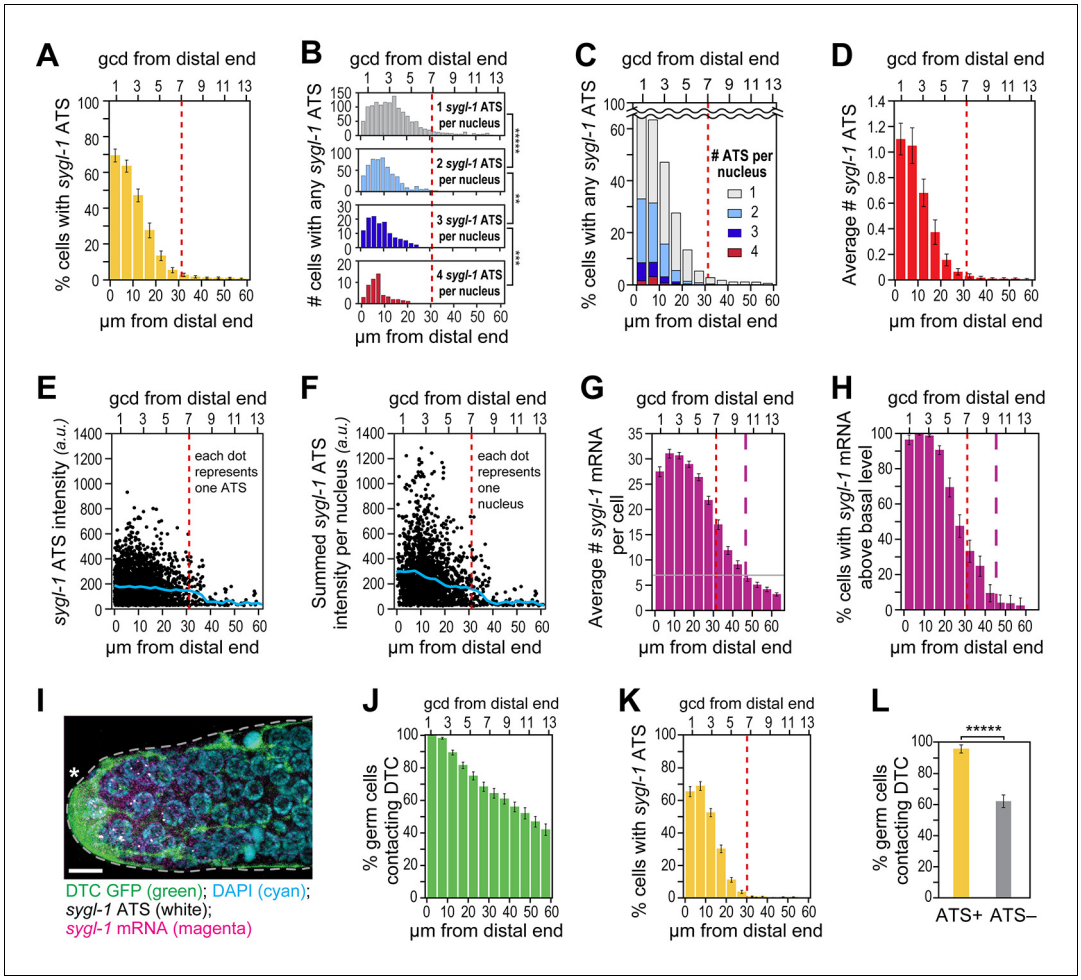

Figure 3. The *sygl-1* transcriptional response is spatially graded. (**A–H** and **K,L**) *sygl-1* smFISH signals as a function of position along the distal-proximal axis of adult gonads. Positions were measured at 5 µm (**A,C–K**) or 2 µm (**B**) intervals from the distal end (x-axis below each graph), and translated to the conventional measure of germ cell diameters (gcd) from the distal end (x-axis above each graph). Error bars: standard error of the mean (SEM). n = 78 gonads. Red dashed line marks the site where the mean percentage of ATS-positive germ cells falls lower than 5%; purple dashed line marks the site where the mean percentage of mRNA-positive germ cells falls lower than 5%. (**A**) Gradient in percentage of germ cell nuclei with any number of *sygl-1* ATS as a function of distance from the distal end in the wild-type adult gonad. By contrast, that percentage is essentially uniform in *glp-1(gf)* gonads (***Figure 3—figure supplement 1A***). (**B**) Numbers of cells with one, two, three or four *sygl-1* ATS per nucleus as a function of distance from distal end. Total n = 2058 nuclei. **p<0.01, ***p<0.001, *****p<0.00001 by t-test. (**C**) Percentages of total ATS-positive nuclei that have one, two, three or four *sygl-1* ATS per nucleus as a function of distance from distal end. Total n = 2058 nuclei. (**D**) Average number of *sygl-1* ATS as a function of distance from the distal end. (**E**) Signal intensities of individual *sygl-1* ATS do not change substantially in region of graded ATS (1–7 gcd, border marked with red line). Each dot represents a single *sygl-1* ATS. The blue curve indicates mean ATS intensity. n = 2978 ATS. Signal intensities of individual *sygl-1* ATS are comparable in *glp-1(gf)* gonads (***Figure 3—figure supplement 1B***). (**F**) Summed *sygl-1* ATS intensities per nucleus were used as a measure for total *sygl-1* nascent transcripts per nucleus and then plotted as a function of distance from the distal end, with each dot representing a single nucleus. The blue curve shows the mean for summed ATS intensities at each position relative to the distal end. n = 2058 nuclei. (**G**) The number of *sygl-1* cytoplasmic mRNA per cell as a function of distance from the distal end. Boundaries of cells were estimated using 3-D Voronoi diagram (***Figure 3—figure supplement 2A***; see Materials and methods for details). The grey line marks the average basal *sygl-1* mRNA level, which was calculated by averaging *sygl-1* mRNA density over a region where mRNAs are both least abundant and no longer graded (the 40–60 µm interval in each gonadal image). A cell with abundant *sygl-1* mRNA can reside next to a cell with few mRNA (***Figure 3—figure supplement 2B–E***). (**H**) Percentage of germ cells with *sygl-1* cytoplasmic mRNAs above basal level as a function of distance from the distal end. (**I**) *sygl-1*

Figure 3 continued on next page

Figure 3 continued

smFISH in adult distal gonad with DTC and its processes visualized with myristoylated GFP (green) and nuclei seen with DAPI (blue). *sygl-1* exon probes mark cytoplasmic mRNAs (magenta) and intron probes (yellow) highlight ATS. Overlap is in white. Conventions and scale as in ***Figure 1E***. Z-projection is shown. (**J-L**) Quantitative analyses of *sygl-1* response in animals where DTC was marked with myristoylated GFP, n = 60 gonads at 24 hr post mid-L4 stage. Error bar: SEM. (**J**) Percentage of germ cells in contact with DTC or its processes as a function of distance from the distal end. (**K**) Percentage of germ cells with one or more *sygl-1* ATS as a function of distance from the distal end. Red dashed line marks region defined as in ***Figure 3A***. (**L**) Percentage of germ cells in contact with DTC or its processes within 30 μm from the distal end. Left bar, ATS-positive cells; right bar, ATS-negative cells or without ATS. *****p<0.00001 by chi-square test for independence.

DOI: 10.7554/eLife.18370.007

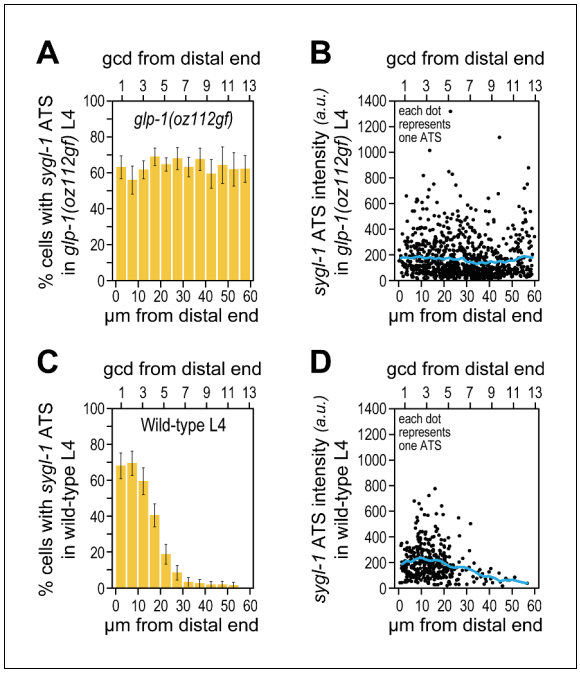

Figure 3—figure supplement 1. The *sygl-1* transcriptional response is not spatially graded in *glp-1 (oz112gf)* mutant germ cells. (**A**,**B**) 3528 nuclei from 10 *glp-1(oz112 gf)* late larval (mid-L4) gonads were used for this analysis. Adult *glp-1(GF)* were not assayed here, because their distal germlines are mitotically quiescent and therefore not similar to wild type. (**C**,**D**) 1902 nuclei from 24 wild-type (mid-L4) gonads were used. (**A**,**C**) Percentage of germ cell nuclei with any *sygl-1* ATS as a function of distance from distal end in *glp-1(oz112 gf)* (**A**) or wild type (**C**). (**B**,**D**) Intensities of individual *sygl-1* ATS as a function of position in *glp-1(oz112 gf)* (**B**) or wild type (**D**), as in ***Figure 3E***.
DOI: 10.7554/eLife.18370.008

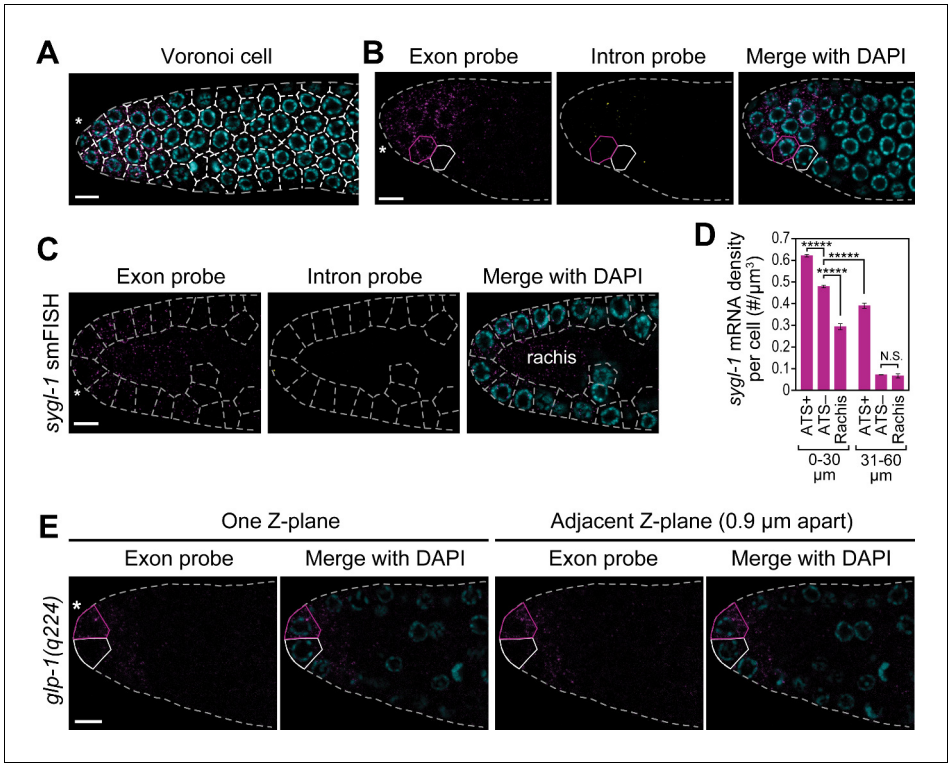

Figure 3—figure supplement 2. Cells with abundant *sygl-1* mRNA can reside next to cells with little mRNA. (**A**,**C**) Germ cells are interconnected via cytoplasmic bridges to a central cytoplasmic core or 'rachis' that extends the length of the gonad (***Hirsh et al., 1976***). Germ cell boundaries (dashed lines) were determined using a 3-D Voronoi diagram (***Ledoux, 2007***; ***Yan et al., 2010***) in MATLAB. A representative section of germ cell boundaries (Voronoi cells) in one Z-plane is shown. DAPI marks nuclei (blue). Conventions and scales as in ***Figure 1E***. (**B**,**E**) Germ cells with abundant *sygl-1* mRNA (magenta outline) can reside next to a neighbor with very little *sygl-1* mRNA (white outline) in wild-type (**B**) or *glp-1(q224)* (**E**) adult gonad. Conventions and scale as in ***Figure 1E***. One Z-plane is shown. (**D**) *sygl-1* mRNA density (total number of mRNAs in cell or region divided by total cytoplasmic volume in same cell or region). Cytoplasmic volume excludes nuclear volume; volume in rachis was calculated from non-cellular germline tissue in region spanning 0–20 μm (4–5 gcd). *****p<0.00001; n.s.: not significant by t-test.
DOI: 10.7554/eLife.18370.009

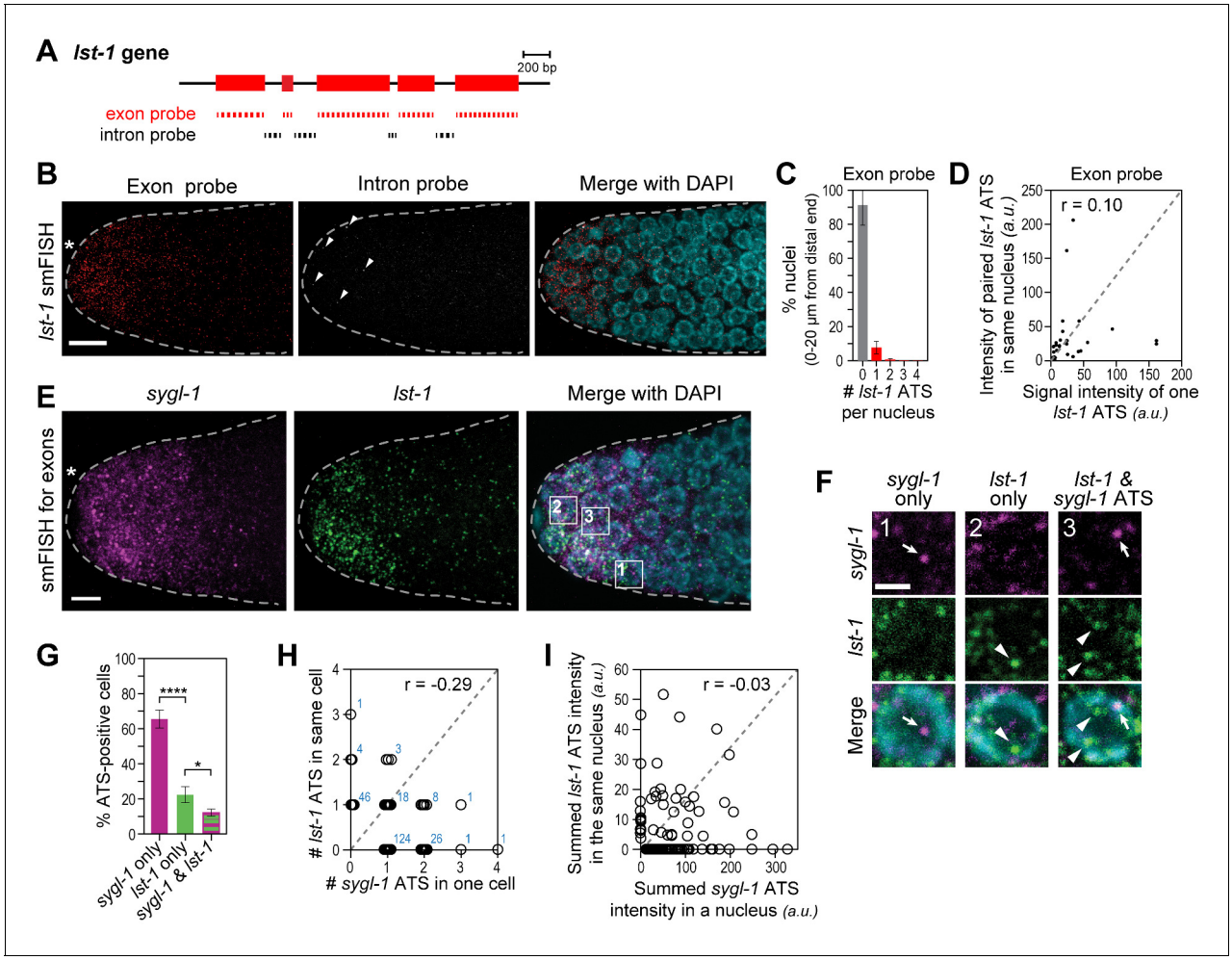

Figure 4. The *lst-1* transcriptional response to Notch signaling. (**A**) Schematic of *lst-1* exon/intron structure. Exon-specific (red) and intron-specific (black) smFISH probes were labeled with different fluors (see Materials and methods). (**B**) *lst-1* smFISH in distal gonad. Exon probes (red); intron probes (white). DAPI marks nuclei (blue). Arrowheads indicate ATS. Conventions and scale as in ***Figure 1E***. (**C**) Percentage of nuclei with 0–4 *lst-1* ATS per nucleus, calculated from 2107 nuclei in 36 gonads: 162 nuclei had one ATS, 15 had two ATS, 3 had three ATS and 2 had four ATS. Error bars: standard deviation. (**D**) Pair-wise comparisons of *lst-1* ATS intensities within one nucleus (total of 30 ATS from 36 gonads). Each black dot represents one pairing. Grey dashed line indicates a perfect correlation (Pearson's correlation coefficient r = 1); r indicates correlation coefficient from data. (**E**) Double-labeled smFISH against *sygl-1* (magenta) and *lst-1* (green) exons using distinct fluors (see Materials and methods). Conventions and scale as in ***Figure 1E***. Full Z-projection is shown. (**F**) 10X magnification of nuclei within boxes in ***Figure 4E***, right panel. Each panel shows a restricted Z-projection that only includes the corresponding nucleus. Arrow: *sygl-1* ATS; arrowhead: *lst-1* ATS. Scale bar: 2 µm. (**G**) Percentage of cells with *sygl-1* ATS only, *lst-1* ATS only or both *sygl-1* and *lst-1* ATS, out of all ATS-positive cells identified (n = 233 cells from 15 gonads). ****p-value<0.0001 and *p<0.05 by t-test. (**H**) Plot of nuclei possessing both *sygl-1* and *lst-1* ATS, with each open circle representing one nucleus (n = 233; 15 gonads). Overlapping data points (open circles) are spread using 'jitter' function in MATLAB. Blue numbers show how many nuclei of each type were found. For example, three nuclei had two *lst-1* ATS and one *sygl-1* ATS. Pearson's correlation coefficient (**r**) is shown on top. Grey dashed line indicates a perfect correlation (r = 1). (**I**) Comparison of summed ATS intensities of *sygl-1* and *lst-1* within the same nucleus (data from 128 nuclei in 9 gonads). Each open circle represents a nucleus. r indicates Pearson's correlation coefficient from data. Grey dashed line indicates a perfect correlation (r = 1).

DOI: 10.7554/eLife.18370.010

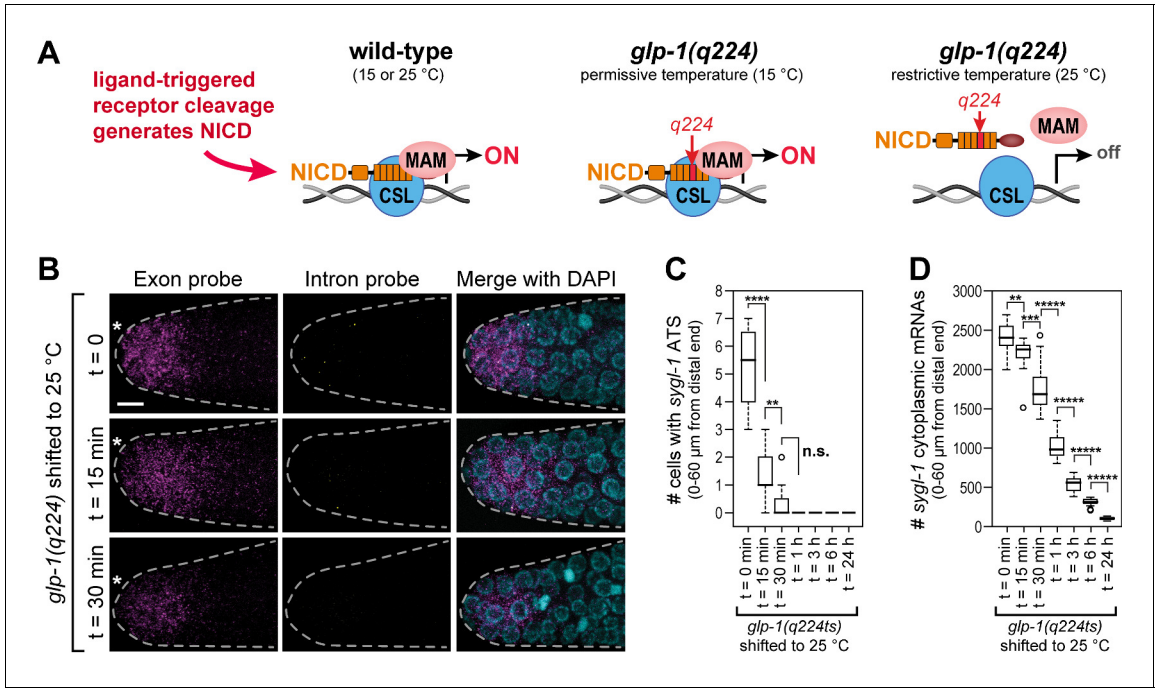

Figure 5. The *sygl-1* transcriptional response is abolished in *glp-1(q224)* mutant germ cells at the restrictive temperature. (**A**) Schematics of GLP-1/Notch-dependent nuclear complex in wild-type and *glp-1(q224)* temperature-sensitive mutant. Left, wild-type GLP-1/Notch intracellular domain (NICD) is cleaved from receptor and assembles into a complex in the nucleus to activate transcription; middle, *glp-1(q224)* NICD has a missense mutation in its fourth ankyrin repeat (red) but can assemble into the complex at the permissive temperature; right, *glp-1(q224)* NICD fails to assemble into the complex at the restrictive temperature. Effect of *glp-1(q224)* on complex formation from ***Petcherski and Kimble (2000)***. CSL, Notch-specific DNA-binding protein; MAM, mastermind-like transcriptional coactivator. (**B-D**) *glp-1(q224)* homozygous adults were raised at the permissive temperature (15˚C) and then shifted to the restrictive temperature (25˚C) for defined time intervals. Dissected gonads were probed for *sygl-1* transcripts with smFISH. n ≥ 20 gonads for each time point. The wild type *sygl-1* transcriptional response is essentially the same at 15, 20 and 25˚C (***Figure 5—figure supplement 1***). (**B**) Z-projections after shift to the restrictive temperature for 0 min (top), 15 min (middle) and 30 min (bottom). *sygl-1* exon probes (magenta); *sygl-1* intron probes (yellow); and DAPI marks nuclei (blue). Conventions and scale as in ***Figure 1E***. (**C,D**) smFISH signals for *sygl-1* ATS (**C**) or mRNAs (**D**) were analyzed in all cells in the region of 0–60 µm (1–13 gcd) from distal end. Asterisks indicate p-value range by t-test. *p<0.05; **p<0.01; ***p<0.001; ****p<0.0001; *****p<0.00001; n.s.: not significant (p>0.05).

DOI: 10.7554/eLife.18370.011

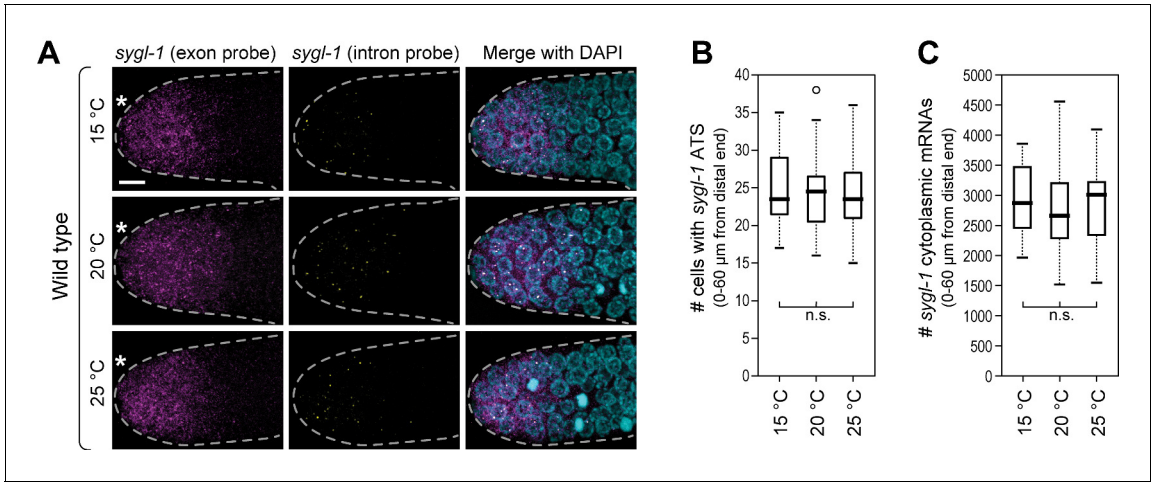

Figure 5—figure supplement 1. Wild-type *sygl-1* transcriptional response is essentially the same at 15, 20 or 25°C. (**A**) Gonads were dissected from wild-type adults raised at 15, 20 or 25°C (hours to adulthood vary at these temperatures; see Materials and methods for staging). Exon probes (magenta); intron probes (ATS; yellow); DAPI marks nuclei (blue). Conventions and scale as in ***Figure 1E***. Z-projection is shown. (**B,C**) Analysis of smFISH signals in germ cells residing 0–60 µm (1–13 gcd) from distal end. n = 16 gonads for each temperature. n.s., not significant (p>0.05) by t-test.
DOI: 10.7554/eLife.18370.012

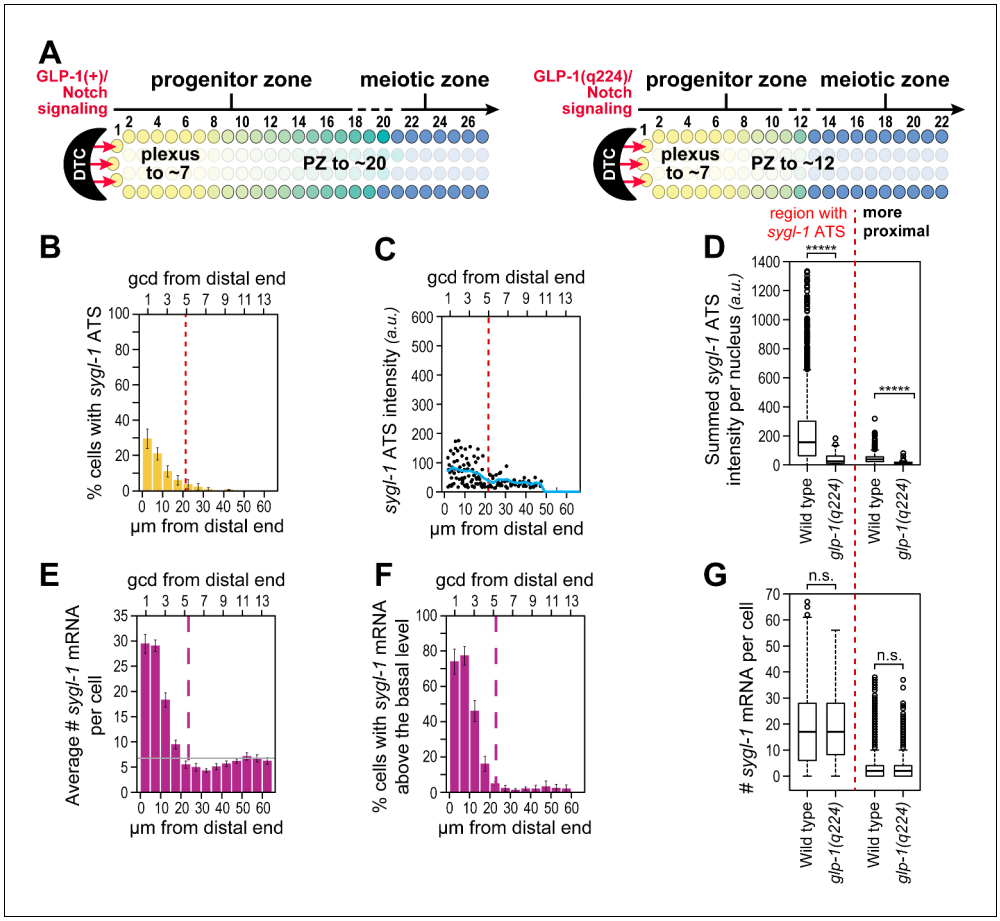

Figure 6. Weakened *sygl-1* transcriptional response in *glp-1(q224)* at permissive temperature. (**A**) The *glp-1(q224)* progenitor zone is smaller than wild-type (***Cinquin et al., 2010***; ***Fox and Schedl, 2015***) though its plexus of DTC processes is essentially the same (***Byrd et al., 2014***). (**B**,**C**,**E**,**F**) *sygl-1* transcriptional response in *glp-1(q224)* at 15°C (n = 20 gonads). Format, conventions and scales as in ***Figure 3A,E,G,H***. (**B**) Percent cells with *sygl-1* ATS as a function of position. (**C**) Individual *sygl-1* ATS intensities as a function of position. (**D**) Summed *sygl-1* ATS intensities per nucleus compared between wild type and *glp-1(q224)*. Left of red line, comparison from region with graded *sygl-1* ATS, which for wild-type was 0–30 µm and for *glp-1(q224)* was 0–20 µm; right of red line, comparison from region proximal to graded *sygl-1* ATS, which for wild-type was 30–60 µm and for *glp-1(q224)* was 20–60 µm. *****p<0.00001 by t-test. (**E**) Average number *sygl-1* mRNAs per cell as a function of position. The grey line marks the average basal *sygl-1* mRNA level (see Materials and methods). (**F**) Percent cells with *sygl-1* mRNAs as a function of position. (**G**) Number of *sygl-1* mRNAs per cell compared between wild type and *glp-1(q224)*. Regions compared were same as described for ***Figure 6D***. n.s.: not significant by t-test.

DOI: 10.7554/eLife.18370.013

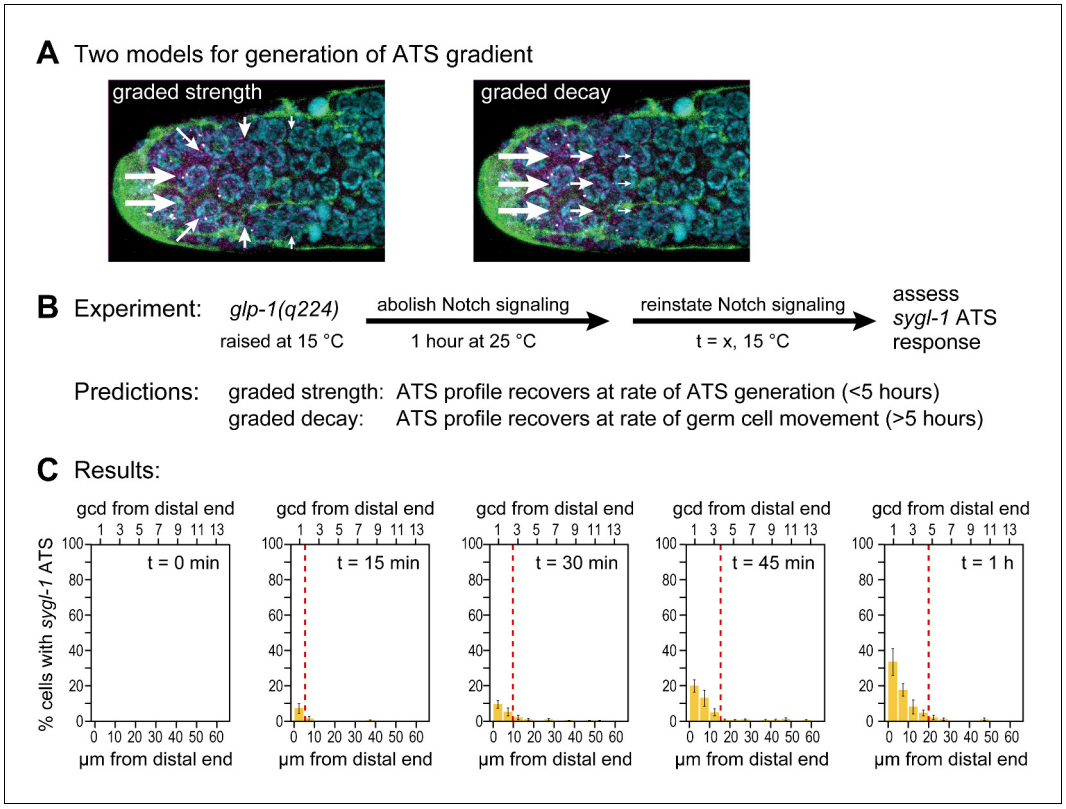

Figure 7. Graded *sygl-1* transcriptional response likely reflects graded signaling strength. (**A**) Two models to generate graded *sygl-1* transcriptional response. Left, DTC signaling is graded within the niche; right, signaling is primarily at distal end but decays as cells move proximally within the niche. (**B**) Above, experiment to monitor rate of ATS pattern establishment after being abolished. Below, prediction made by each model. (**C**) Graded response is re-established within 1 hr. Percentage germ cells with *sygl-1* ATS as a function of distance at 15 min intervals during reformation. Red line marks the region with *sygl-1* ATS, as in ***Figure 3A***. Conventions as in ***Figure 3A***; n = 21 gonads for each time point.

DOI: 10.7554/eLife.18370.014

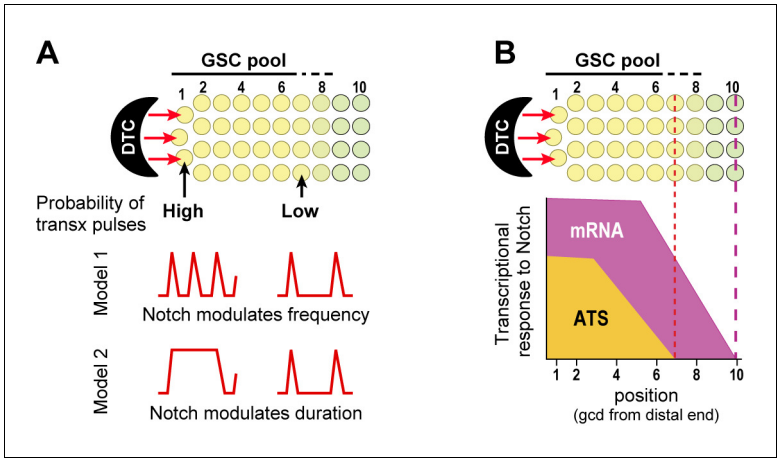

Figure 8. Gradient of Notch-dependent active transcription sites: models for underlying mechanism (**A**) and relation to mRNA distribution (**B**). (**A,B**) Top, Notch signaling from the DTC niche maintains a pool of germline stem cells (GSCs) (***Cinquin et al., 2010***). (**A**) Notch signaling generates a gradient in the probability of transcriptional activation across the stem cell pool. ATS probability differences may result from modulation of ATS frequency (Model 1) or duration (Model 2). Red lines illustrate theoretical effects on transcriptional bursting at high (left) or low (right) probability. (**B**) Notch signaling from niche generates differently-shaped gradients of ATS and mRNA: mRNA abundance is essentially ungraded in the region where ATS probability is graded; the mRNA gradient extends further proximally than the ATS gradient; and more cells have mRNAs than ATS at any given position.

DOI: 10.7554/eLife.18370.015